Science Bulletin 64 (2019) 63–72

Contents lists available at ScienceDirect

Science Bulletin

journal homepage: www.elsevier.com/locate/scib

Review

Towards reliable Arctic sea ice prediction using multivariate data assimilation

Jiping Liu [a,*], Zhiqiang Chen [b], Yongyun Hu [c], Yuanyuan Zhang [d], Yifan Ding [d], Xiao Cheng [d], Qinghua Yang [e], Lars Nerger [f], Gunnar Spreen [g], Radley Horton [h], Jun Inoue [i], Chaoyuan Yang [a], Ming Li [j], Mirong Song [k]

[a] Department of Atmospheric and Environmental Sciences, University at Albany, State University of New York, Albany, NY 12222, USA
[b] College of Ocean and Meteorology, Guangdong Ocean University, Zhanjiang 524088, China
[c] Department of Atmospheric and Oceanic Sciences, School of Physics, Peking University, Beijing 100871, China
[d] College of Global Change and Earth System Science, Beijing Normal University, Beijing 100875, China
[e] Guangdong Province Key Laboratory for Climate Change and Natural Disaster Studies, and School of Atmospheric Sciences, Sun Yat-sen University, Zhuhai 519082, China
[f] Alfred-Wegener-Institut Helmholtz Zentrum für Polar- und Meeresforschung, Bremerhaven 27570, Germany
[g] University of Bremen, Institute of Environmental Physics, Bremen 28359, Germany
[h] Lamont-Doherty Earth Observatory, Columbia University Earth Institute, Palisades, NY 10964, USA
[i] National Institute of Polar Research, Tachikawa 190-8518, Japan
[j] Polar Research and Forecasting Division, National Marine Environmental Forecasting Center, Beijing 100081, China
[k] State Key Laboratory of Numerical Modeling for Atmospheric Sciences and Geophysical Fluid Dynamics, Institute of Atmospheric Physics, Chinese Academy of Sciences, Beijing 100029, China

ARTICLE INFO

Article history:
Received 9 October 2018
Received in revised form 12 November 2018
Accepted 22 November 2018
Available online 29 November 2018

Keywords:
Arctic sea ice prediction
Remote sensing
Data assimilation

ABSTRACT

Rapid declines in Arctic sea ice have captured attention and pose significant challenges to a variety of stakeholders. There is a rising demand for Arctic sea ice prediction at daily to seasonal time scales, which is partly a sea ice initial condition problem. Thus, a multivariate data assimilation that integrates sea ice observations to generate realistic and skillful model initialization is needed to improve predictive skill of Arctic sea ice. Sea ice data assimilation is a relatively new research area. In this review paper, we focus on two challenges for implementing multivariate data assimilation systems for sea ice forecast. First, to address the challenge of limited spatiotemporal coverage and large uncertainties of observations, we discuss sea ice parameters derived from satellite remote sensing that (1) have been utilized for improved model initialization, including concentration, thickness and drift, and (2) are currently under development with the potential for enhancing the predictability of Arctic sea ice, including melt ponds and sea ice leads. Second, to strive to generate the "best" estimate of sea ice initial conditions by combining model simulations/forecasts and observations, we review capabilities and limitations of different data assimilation techniques that have been developed and used to assimilate observed sea ice parameters in dynamical models.

1. Introduction

The Arctic warming is much faster than global warming. Sea ice cover in the Arctic has declined since at least the early 1950s [1,2]. Negative trends in the total Arctic sea ice extent are observed for every month since the late 1970s [3], with the largest decrease in September. The ice extent in September has decreased by 3.24 million km^2 during 1979–2017, with significant ice reduction in the periphery of the Arctic Basin, from the western Beaufort Sea to the northern Kara/Barents Seas (Fig. 1). The observed rate of September sea ice decline is underestimated by most of current day climate models [4]. Accompanying the reduction of the ice cover has been a thinning of the ice pack. Compared to submarine observations during 1958–1976, recent satellite data showed that the mean Arctic sea ice thickness has decreased ~50% [5,6]. This is mainly due to the thinner seasonal ice replacing thicker multi-year ice [7,8]. As a result, Arctic sea ice has tended to be more akin to the marginal ice zone. Sea ice can be disturbed more easily by weather systems and ocean waves, which fracture ice and push ice floes around to create leads and polynyas. Observations of sea ice mass balance buoys and satellites showed that the ice drift speed has increased, which reduces the strength and increases the deformation of sea ice in the Arctic [9–11].

The above mentioned changes of Arctic sea ice have captured attention and pose significant challenges to many stakeholders, including shipping, oil/gas exploration, and coastal communities facing the prospect of relocation [12–15]. As a result, there is an

* Corresponding author.
E-mail address: jliu26@albany.edu (J. Liu).

https://doi.org/10.1016/j.scib.2018.11.018
2095-9273/

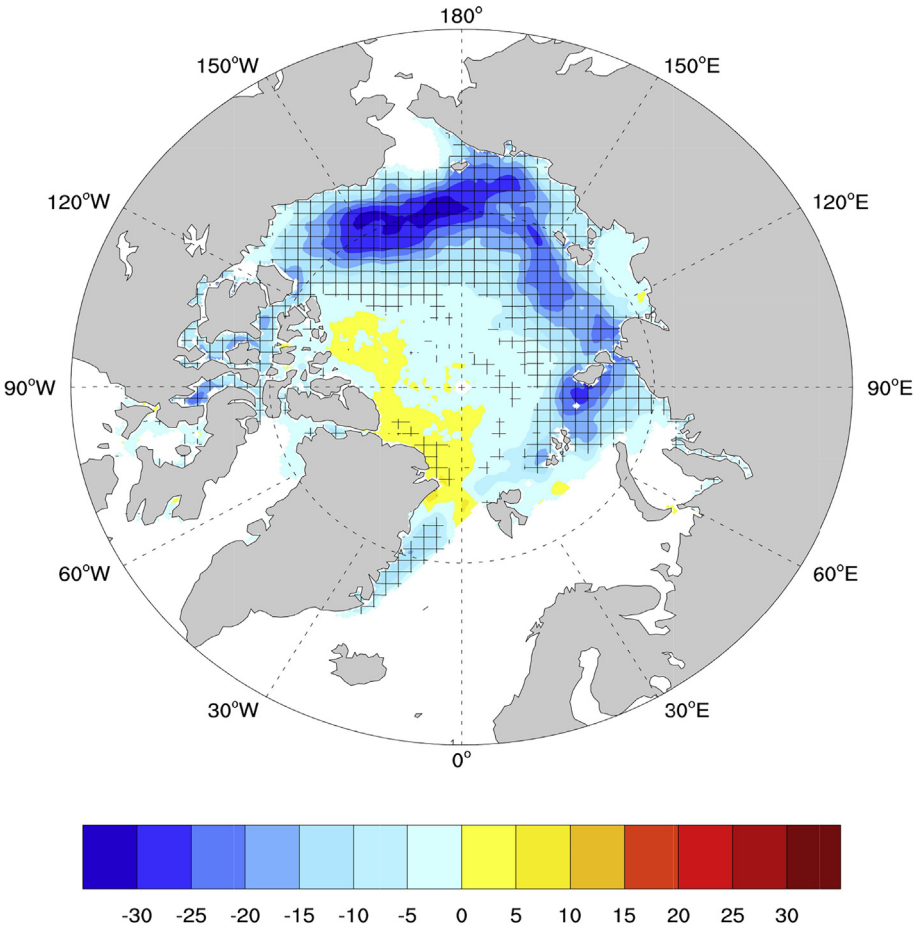

Fig. 1. Linear trends of September sea ice concentration in the Arctic during the period of 1979–2017 (% per decade). The meshed areas denote the trends above 95% confidence level. The data is obtained from the National Snow and Ice Data Center.

increasing need of Arctic sea ice prediction ranging from daily to seasonal time scales [13,16,17], driven in particular by an increasing accessibility of the Arctic associated with global climate change. Moreover, the rapid decline of Arctic sea ice in recent years has coincided with more frequent extreme events in parts of northern mid-latitude continents, i.e., several winters following anomalously low Arctic sea ice cover had strong cold surges along with heavy snowfall [18–23]. Hence accurate Arctic sea ice prediction might have the potential for improving seasonal climate prediction in the northern mid- and high-latitudes. Analyses of climate model projections suggested that Arctic sea ice would continue to decrease and reach an ice-free state in the middle of 21st century associated with global warming [24–27].

Since 2008, a call for sea ice outlook has been announced every year to research community for predictions of seasonal minimum sea ice extent in the Arctic (http://www.arcus.org/sipn), which provides the basis for our knowledge of the progress of Arctic sea ice prediction. During past years, sea ice prediction has been primarily conducted through statistical models. For example, most utilize linear regression models, which are trained with observations in the past, and used to predict future sea ice state. Coupled sea ice-ocean models have been used to predict sea ice cover, which are forced by an ensemble of prescribed atmospheric forcing from numerical weather predictions [28]. Some institutions have also developed operational systems configured for the Arctic region for short-term sea ice forecasts. Examples are the U.S. Navy Arctic Cap Nowcast/Forecast System (ACNFS) [29], the Canadian Regional Ice Prediction System (RIPS) [30], and the TOPAZ4 coupled ocean sea ice data assimilation system [31]. In recent years, major operational and modeling centers have implemented sea ice model components in their global coupled predictive models for sea ice prediction. Examples are the NCEP Climate Forecast System [32], the NASA Goddard Earth Observing System Model [33], and the UK Global Seasonal Forecast System [34]. Sea ice prediction is particularly challenging in the context of coupled predictive models. In the fully coupled predictive model, sea ice strongly interacts with both the atmosphere above and the ocean below. Variation in the ice cover and thickness regionally would influence atmospheric and oceanic conditions, which in turn affect sea ice distribution (concentration and thickness). The ongoing subseasonal-to-seasonal (S2S) project provides opportunities to compare the operational sea ice forecast conducted by major operational and modeling centers (http://gpvjma.ccs.hpcc.jp/S2S/S2S_SICmap.html).

Fig. 2 shows the median and interquartile range of the predicted September sea ice extent obtained from the July outlook by dynamical models, including coupled sea ice-ocean models, and fully coupled Arctic and global models. It appears that the median sea ice predictions for most years deviate from the observations substantially, for example in the record-low year of 2012. So far, the predictive skill of seasonal minimum ice extent by numerical models is generally comparable to that of statistical methods. Clearly, seasonal Arctic sea ice prediction remains challenging. It is well known that dynamic models used to predict Arctic sea ice at short-term periods strongly depend on model initial conditions. Thus, a multivariate data assimilation that assimilates sea ice

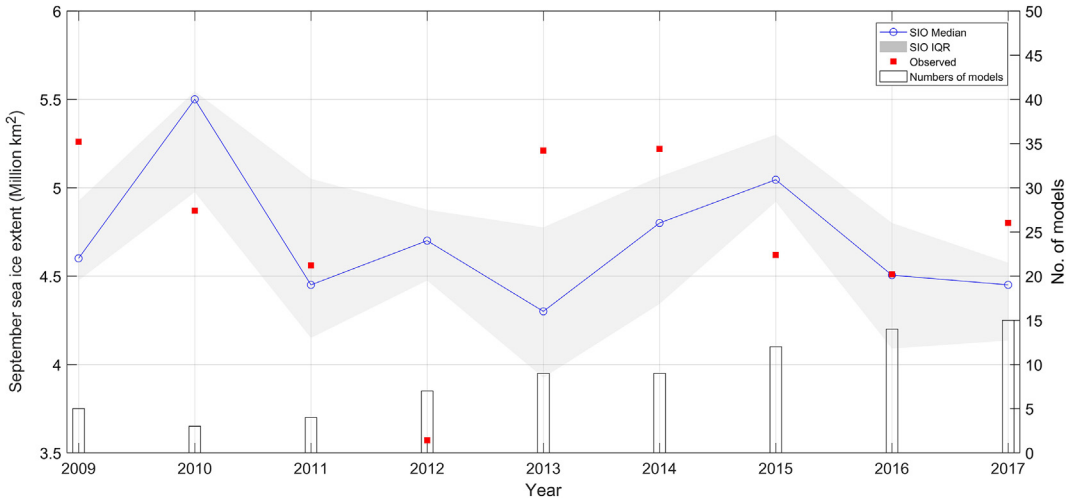

Fig. 2. The median and interquartile range of the predicted September sea ice extent based on July outlook by dynamical models that are participated in the Sea Ice Prediction Network. *Y*-axis: left is September sea ice extent and right is the number of dynamical models.

observations to generate realistic and skillful model initialization is needed to improve Arctic sea ice prediction.

Observations are of course essential inputs for the multivariate data assimilation. However, observations in the Arctic have limited spatiotemporal coverage and large uncertainties. In Section 2, we discuss satellite remote sensing of sea ice parameters that (1) have been utilized and (2) are currently under development for improved model initialization, which could enhance the predictability of Arctic sea ice at daily to seasonal time scales. To reduce uncertainties associated with sea ice initial conditions that are based on imperfect representations of physical processes by dynamical models, data assimilation techniques have been utilized to assimilate various observed sea ice parameters in dynamical models. However, it is not clear which data assimilation method is the best choice to generate the "best" estimate of sea ice initial conditions by combining model simulations/forecasts and observations. In Section 3, we review the capabilities, and limitations of different data assimilation methods.

2. Satellite remote sensing of sea ice parameters

The evolution of Arctic sea ice during the melting season is strongly determined by characteristics of initial ice conditions, which affect subsequent thermodynamic and dynamic sea ice change. Thermodynamic changes consist of surface, internal, lateral and bottom melts, and dynamic changes include transport and deformation. Hence predictability of Arctic sea ice from days to seasons strongly depends on the initial sea ice state [35,36]. Here we review sea ice parameters derived from satellite remote sensing that would aid in sea ice prediction procedures.

2.1. Sea ice concentration

To date, sea ice concentration data used to improve model initialization are primarily based on the retrievals using brightness temperature from passive microwave radiometers, including the Scanning Multi-channel Microwave Radiometer (SMMR), Special Sensor Microwave/Imager (SSM/I), Special Sensor Microwave Imager/Sounder (SSMIS), Advanced Microwave Scanning Radiometer for EOS (AMSRE), and AMSR2. A variety of retrieval algorithms have been proposed (see Refs. [37,38] for detailed comparisons of algorithms). These algorithms use different channel combinations of brightness temperature to distinguish sea ice and open water, as well as make different corrections (i.e., weather filters, satellite drifts). Table S1 (online) provides a summary and snapshot of available near real-time satellite-based sea ice concentration data sets [39–44]. These data sets can be assimilated as the "best" estimate of the initial ice coverage for operational sea ice forecast in coupled predictive models. The horizontal resolution of SSMIS-based (25–10 km) and AMSR2-based (15–5 km) data sets is approximately comparable to most of current global and regional Arctic prediction systems, respectively. However, as the resolution of regional Arctic prediction systems increases over time, the need for higher resolution satellite sea ice concentration grows. Concepts for radiometers with larger antenna reflectors for higher spatial resolution are currently developed (e.g., Copernicus CIMR).

A number of studies have leveraged the extensive coverage of sea ice concentration (both spatially and temporally) to examine the assimilation of satellite-based ice fraction in stand-alone sea ice models [45–48], sea ice-ocean coupled models [49–55], and fully coupled climate models [56–58]. These studies demonstrated that assimilating sea ice fraction successfully reduces the models' bias and significantly improves the predictive skill of regional distribution of the ice cover and the total ice extent. Ivanova et al. [37] pointed out that sea ice concentration obtained from the same passive microwave product but with different retrieval methods can lead to a difference in the total Arctic sea ice extent (area) up to 0.6 (1.3) million km^2, particularly during the melting season associated with changing surface features of sea ice (i.e., wet snow, ponds). Hindcasts/predictions that differ only in the assimilated products of sea ice fraction as the estimate of the initial condition show increasing discrepancies in the simulated Arctic sea ice extent/area. This further leads to significant differences in seasonal climate prediction [59]. Thus, data assimilation needs both observations of sea ice concentration and their uncertainty estimates. In general, the studies as mentioned above assume the uncertainty of observed sea ice concentration to be constant, i.e., 15% is typically used to represent observational error [60]. A recent study showed that using satellite-based sea ice concentration with appropriate uncertainty estimates can improve the ensemble mean forecast of ice fraction in a sea ice-ocean coupled model compared to that with constant uncertainty, but the ice thickness forecast appears to be degraded [61]. Hence there is scope for further improvement by using realistic varying uncertainty estimates of observed sea ice concentration (both spatially and temporally), i.e., the recently released sea ice concentration under the ESA-CCI sea ice project (SICCI) provides quantitative information on uncer-

tainty induced by the algorithm and spatial remapping, which is helpful for sea ice assimilation [62]. Additionally, some studies noted that assimilating observed sea ice concentration yields little reduction of the models' bias in sea ice thickness.

2.2. Sea ice drift

Sea ice drift caused by winds and ocean currents strongly influences ice concentration and thickness, i.e., divergence of the ice pack creates open water, where new ice grows in winter and the lateral melt increases in summer, and convergence of the ice pack increases ice concentration and thickens the ice by rafting/ridging. Using satellite and buoy observations, Olason and Notz [63] showed that variation in the ice motion is strongly associated with variation in ice conditions, i.e., for low ice fraction, drift speed generally increases with reducing concentration, while for high ice fraction, drift speed is more closely associated with thickness. As mentioned previously, the ice strength of in the Arctic has been reduced due to the decrease of the ice cover and thickness. This allows more deformation, and then increases the movement of sea ice. Several hemispheric wide sea ice drift data sets have been developed primarily based on brightness temperature measured by passive microwave radiometers and scatterometers, including SMMR, SSM/I, SSMIS, AMSR-E, AMSR2, QuikSCAT, and Advanced Scatterometer (ASCAT) [64–66]. For regional studies, sea ice drift data from Synthetic Aperture Radar (SAR) provide higher resolution and accuracy [67,68]. In general, the ice drift is derived from the movement of ice floes in a certain time interval using continuous satellite imagery [69]. Table S2 (online) provides a summary and snapshot of near real-time gridded sea ice drift data sets that can be assimilated as the estimate of the initial condition for operational sea ice forecast in coupled predictive models [70,71]. Despite the low spatial resolution, a recent uncertainty estimate [72] suggested that OSI SAF data, which combines the brightness temperature from SSMIS, AMSR2 and ASCAT, might have better quality compared to other ice drift data.

Research has examined the incorporation of observed sea ice motion in stand-alone sea ice models [48,73–78], and sea ice-ocean coupled models [79]. Their results showed that the simulation of sea ice circulation is substantially improved as the ice drift data is assimilated, in particular the response of the ice motion to weather systems. A few studies suggested that assimilating the ice drift data also has a strong impact on the simulation of sea ice concentration as well as thickness, which in turn affects the ice motion. Thus a high quality observation of sea ice drift would aid in sea ice forecast procedure. Currently, most of the available sea ice drift data sets do not provide uncertainty estimates for the ice displacement in each grid cell, but only provide the mean value for all ice displacements. Compared with buoy data and synthetic aperture radar images, recent studies suggested that the ice drift speed error is dependent on its magnitude, and the error in summer is two times larger than that of winter [72,79]. Thus a thorough error assessment of these data sets (i.e., uncertainty maps for different sea ice conditions) is needed to understand effects of uncertainties in satellite-derived sea ice drift on predictive skill of Arctic sea ice. The representation of ice dynamics especially sea ice deformation in sea ice models needs further attention. With current viscous-plastic model ice rheologies, high resolution (<10 km) models are needed for a more realistic ice deformation representation [80]. Alternative ice rheologies like elasto-brittle are currently developed and might help a more realistic representation of sea ice dynamics [81].

In the past two to three decades, most efforts have been made to assimilate observed sea ice concentration and drift in dynamical models. For better Arctic sea ice prediction, besides accurate sea ice concentration and drift, model initialization also needs sea ice parameters that modulate energy fluxes at atmosphere-sea ice-ocean interface [35,82]. These additional variables are discussed below.

2.3. Sea ice thickness

Recent studies showed that anomalies of sea ice thickness could persist much longer than that of sea ice cover. The preconditioning of the ice thickness has been shown to be important for Arctic sea ice prediction at longer time scales [35,83–86]. However, compared to sea ice concentration, it is difficult to observing sea ice thickness from space [87,88]. In recent years, many efforts have been underway to generate basin-scale sea ice thickness data from satellites. The CryoSat2 satellite radar altimeter provides observations of sea ice thickness, which extends the 2003–2008 ICESat thickness record post-2010. Sea ice thickness is retrieved from the ice freeboard measurements by CryoSat2 along with a climatological estimate of snow depth and density [88]. The uncertainties of the CryoSat2 ice thickness mainly originate from the inadequate knowledge of snow depth and density of snow/ice, the freeboard determination itself that is needed for the conversion from freeboard to ice thickness, and the radar interaction with snow [89,90]. Thus, the accurate observation of snow depth is important for sea ice thickness retrieval, but the retrieval of snow depth over sea ice and the assessment of its variability are a challenging work [91,92]. CryoSat2-derived sea ice thickness is more accurate for thick and perennial ice. The Soil Moisture and Ocean Salinity (SMOS) satellite radiometer, on the other hand, provides brightness temperature measured at L-band (1.4 GHz) microwave frequency that is utilized to derive the thickness for thin ice (relatively deeper penetration in snow/ice). It has been used to derive sea ice thickness using a single layer emissivity model at close to nadir observations [93,94], and an empirical model based on polarization difference at 40°–50° incidence angle [95]. Recently observations from the NASA SMAP L-band radiometer were also used for thin ice thickness retrieval and combined with SMOS data [96,97], which will increase the number of observations per day and make the retrieval more robust. The maximum retrievable ice thickness from microwave radiometers depends on the penetration depth, which saturates at about 50–100 cm for L-band. Uncertainties increase for thicker ice when small brightness temperature changes relate to large ice thickness changes [93–95]. Further uncertainty contributions stem from sub-footprint surface type variability (i.e., can be large for the SMOS 40 km footprint), brightness temperature measurement, auxiliary datasets, and assumptions made in the retrieval algorithm. More recently, Ricker et al. [98] has developed a merged product of CryoSat2 and SMOS data by taking advantage of their complementary features. The data is merged weekly to take into account different temporal resolutions of the CryoSat2 and SMOS data (note that this product is only available until 2017). With faster and more precise lasers, the recently lunched NASA's Ice, Cloud and land Elevation Satellite 2 (ICESat2) will provide even more precise and uniform coverage of sea ice thickness observations. Table S3 (online) provides a summary and snapshot of the available gridded satellite sea ice thickness products that can be assimilated in coupled predictive models when selecting initial conditions for operational sea ice forecasts [88,95,99–102].

Unlike sea ice concentration, there are limited studies that investigate impacts of sea ice thickness assimilation. A few studies examined the potential influence of assimilating the aforementioned satellite-derived sea ice thickness in sea ice-ocean coupled models [103–109]. They found that the assimilation of the ice thickness has an obvious impact on the simulated sea ice fields, leading to significant reduction in the bias of the modeled ice thickness for several months. Collow et al. [110] and Chen et al.

[111], respectively, have assimilated sea ice thickness from the Pan-Arctic Ice Ocean Modeling and Assimilation System (PIOMAS, an Arctic sea ice reanalysis [112]) and the combined CryoSat2 and SMOS retrievals, in the NCEP Climate Forecast System. The results showed that the experiment assimilating ice thickness results in a significant reduction of systematic bias in the forecasted ice thickness relative to the experiment assimilating ice concentration only or without sea ice assimilation. Moreover, they pointed out that assimilating both sea ice thickness and fraction benefits the prediction of sea ice concentration in distinct regions as well as interannual variability. This is primarily due to the covariability between sea ice thickness and concentration. Hence a high quality measurement of sea ice thickness would aid in sea ice forecast procedure. Research is also needed to understand sensitivity of predictive skill of Arctic sea ice to uncertainties in satellite-derived sea ice thickness, i.e., how the impacts of a given thickness error on forecast skill may differ by month and location. The aforementioned merged product of CryoSat2 and SMOS and recently released SICCI sea ice thickness provide quantitative information on uncertainty that is helpful for sea ice assimilation. Additionally, a few efforts are underway to improve estimate of Arctic-wide sea ice thickness/volume and Arctic reanalysis by assimilating the combined CryoSat2 and SMOS sea ice thickness [113,114].

2.4. Melt pond fraction

During the melting season, as snow/ice melts, ponds form as melt water accumulates on the surface. The area and depth of melt ponds depends on surface topography and ice internal structure [115,116]. First-year ice is on average less deformed than multi-year ice, and thus a high surface fraction of first-year ice is covered by melt ponds in summer. The albedo of the ponds is much smaller than snow and bare ice. Surface albedo decreases as more melt water accumulates on the ice, which absorbs more solar radiation and further melts snow/ice [117–119]. Light measurements under summer Arctic sea ice showed that first-year ice covered by ponds allows nearly a factor of three more insolation to pass through the ice than multi-year ice [120,121]. Thus larger pond coverage leads to higher fraction of solar radiation being transmitted through sea ice during the melt season, enhancing the ice melt, leading to a positive albedo-transmittance-melt feedback [118,122]. A recent modeling study suggested that considering melt ponds might improve the skill of seasonal Arctic sea ice prediction [123]. A parallel study using satellite observations further showed that a integration of pond fraction from late spring to mid-summer strongly influences sea ice variation during the melting season, which can improve the prediction of seasonal minimum sea ice extent [124]. Thus the assimilation of pond fraction observations has the potential to improve Arctic sea ice prediction. However, to date, melt ponds have not been assimilated to improve the initial sea ice condition due to a lack of accurate basin wide melt ponds observations.

Recently, some efforts have been underway to generate basin-wide melt pond fraction data from satellites. Using a neural network, Rösel et al. [125] retrieved the pond fraction from surface reflectance data measured by the Moderate Resolution Image Spectroradiometer (MODIS). The method takes into account that freshwater ponds have different spectral features compared to snow/ice and open water. Zege et al. [126] and Istomina et al. [127] retrieved melt pond fraction using the Medium Resolution Imaging Spectrometer (MERIS) radiance coefficients as well as solar and observation angles. The method employs an analytical solution of sea ice surface reflection and a radiative transfer model, instead of a priori reflectance of different ice types. This method along with a recently improved forward model [128] is being applied to Sentinel-3 data for improved detection of melt ponds. The above MODIS and MERIS based melt ponds fraction products are only available until 2011 (https://icdc.cen.uni-hamburg.de/1/daten/cryosphere/arctic-meltponds.html and https://seaice.uni-bremen.de/melt-ponds). Recently, following the similar approach in Ref. [125] but with some improvements, the MODIS melt ponds data set has been extended to present and validated that can be assimilated in coupled predictive models for operational sea ice forecasts (see Table S4 online for details). Current melt pond satellite retrievals are based on optical data, which is hampered by clouds. Hemispheric-wide melt pond fraction maps can only be derived by accumulating data over at least one week. This introduces uncertainties in the detection of melt onset, melt pond cover development and freeze-up date. In future, it will be important to assess how such uncertainties in the pond fraction retrievals, which vary by month and location impact Arctic sea ice prediction.

2.5. Sea ice leads

Sea ice leads are narrow and non-linear cracks in the ice pack resulting from the deformation of sea ice and upwelling of warm water. Leads are important sites of heat, salt and gas fluxes that strongly influence Arctic sea ice variation, although the total area of leads is relatively small. Sea ice leads result in large variation in surface temperature and thus sensible and latent heat fluxes [129–131]. Leads have lower reflectivity compared to the surrounding ice, resulting in enhanced absorption of solar radiation during the melting season. This warms the water in leads and enhances sea ice melt, especially lateral melt, that creates more openings, and thus allows more heat to the atmosphere [132]. Sea ice deformation related to leads is also important for marine operations in the Arctic Ocean. A recent analysis based on satellite-derived sea ice leads shows that an integrated the lead area from January to April is a good predictor of July sea ice cover [133]. Thus the assimilation of leads (e.g., the areal coverage) into coupled predictive models can potentially improve the skill of sea ice prediction. However, sea ice leads are rarely used for model initialization because of two issues. First, leads are underrepresented process in sea ice prediction systems because of their small-scale and irregular occurrence characteristics. Only newer ice rheologies can adequately use them for initialization [81]. Second, there is a lack of accurate basin wide sea ice leads observations.

Recently, a few efforts have been made to retrieve sea ice leads from satellites. Röhrs and Kaleschke [134] applied an algorithm to the AMSR-E passive microwave brightness temperature to obtain leads at least 3 km in width. Willmes and Heinemann [135,136] derived sea ice leads composite maps by applying a binary segmentation procedure to the MODIS ice surface temperature product, detecting significant positive surface temperature anomalies associated with leads. They also used a spatiotemporal cloud artifact filter to identify physical leads and remove cloud artifacts due to the uncertainty of the MODIS-based cloud mask. This provides the possibility to obtain sea ice leads information continuously from the MODIS data. The MODIS sea ice leads product is only available until 2015 [136]. Recently, following the approach developed by Ref. [135] but with different filter windows, MODIS sea ice leads data set has been extended to present and validated that can be assimilated in high-resolution coupled predictive models for operational sea ice forecasts (see Table S5 online for details).

3. Data assimilation methods

Data assimilation combines sea ice observations, numerical models, and their error statistics to create an improved model initialization in a physically consistent manner, which enhances the predictive skill for sea ice. Different methods have been imple-

mented to assimilate some of the aforementioned sea ice parameters in a hierarchy of models used for Arctic sea ice simulation and prediction. These methods include nudging, optimal interpolation, variational methods, and ensemble Kalman filters. Here a summary of these methods is provided, demonstrating how they work, how they are different, what advantages and disadvantages they have, and what improvements can be expected over time.

(1) Nudging is the simplest method (also called Newtonian relaxation). It uses the difference between the modeled or background (x_b) and observed (y_o) sea ice field (i.e., $\Delta x = x_b - y_o$) to correct the modeled state, so that $x_a = x_b - \alpha\Delta x$, where x_a is the analyzed sea ice field, and α is the empirically determined nudging factor. The nudging is applied during the time stepping of the model and pulls the modeled sea ice field towards the observations. Nudging is easy to implement and has vey low computational cost. It has been utilized to update the modeled sea ice concentration towards the observations in sea ice-ocean coupled models [50,51] and in coupled global climate model [57]. Other modeled sea ice and related variables (i.e., sea ice thickness, sea surface temperature) are then adjusted to be consistent with the updated ice concentration, i.e., the update of the ice thickness is set to be proportional to the updated ice concentration [57]. Recently, nudging has been used to assimilate CryoSat2 sea ice thickness in the Met Office's coupled seasonal forecasting system [137]. The results of these studies suggested that the simple nudging approach is useful for generating skillful sea ice initialization, which results in improved sea ice simulation. However, nudging does not consider spatial correlation in the modeled and observed sea ice fields, and multivariate covariances, which leads to dynamical inconsistencies. A more objective method that takes into account observation and model error statistics is needed, i.e., optimal interpolation.

(2) Optimal Interpolation (OI) determines the optimal weight matrix (W) that minimizes the estimated error covariance of the observed and modeled sea ice field, as described by the following equations.

$$x_a = x_b + W[y_o - H(x_b)],$$

$$W = BH^T\left(HBH^T + R\right)^{-1},$$

where B is the background (model) error covariance matrix, which determines the filtering of sea ice observations and its propagation to the model space, and R is the observation error covariance matrix. H sets the relationship between the model and the observed sea ice variables (called observation operator). The OI solves the equation directly by inverting the matrix $HB + R$. The OI has been used to assimilate satellite sea ice concentration in the Regional Ocean Modeling System [56] and the ECHAM5/MPI-OM climate model [57], which significantly reduces the difference in the ice fraction and extent between simulations and observations. The OI has also been used to examine impacts of assimilating observed sea ice drift in stand-alone sea ice models [73–77] and a sea ice-ocean coupled model [79]. These studies noted significant improvements in the simulation of sea ice circulation, but mixed or degraded performance in other modeled sea ice variables (i.e., sea ice thickness). This is in part due to the incorporation of observed sea ice drift tends to violate the ice dynamics in the model [77]. A few studies further investigated the most appropriate way to assimilate both sea ice drift and concentration in coupled ice-ocean models using the OI [48,52]. They suggested that assimilating ice drift and concentration could be complementary, since the former (latter) is mainly dynamically driven (thermodynamically controlled). However, the corrected sea ice state obtained from the OI is still not consistent with model dynamics due to (1) error statistics determined by some simplified assumptions and (2) artifacts introduced by restricting observations falling in a surrounding area of each model grid cell, which limits us to simple observation operators. Thus there is a tendency towards variational methods.

(3) The three dimensional variational method (3DVAR) bases on optimal control theory, in which a cost function is minimized under dynamical constraints that satisfy the governing equations of the model [138]. The cost function $J(x)$ is given by

$$J(x_a) = \frac{1}{2}(x_a - x_b)^T B^{-1}(x_a - x_b) + \frac{1}{2}\left[y_o - H(x_b)^T\right]R^{-1}[y_o - H(x_b)].$$

Let the gradient $\nabla J(x) = 0$, then

$$x_a = x_b + \left(B^{-1} + H^T R^{-1} H\right)^{-1} H^T R^{-1}[y_o - H(x_b)].$$

In practice, the analyzed sea ice state is obtained through minimizing the cost function using iterative methods. It represents the maximum likelihood estimate of the true sea ice state given the error information from two sources (background and observation). 3DVAR takes into account all available observations, which avoids the selective data used in the OI. In general, 3DVAR assumes that the error covariance matrix is stationary. It has been demonstrated that 3DVAR is effective at generating improved sea ice initial conditions, leading to more skillful forecasts in sea ice-ocean coupled models [55,139]. Currently, the U.S. Navy Arctic Cap Nowcast/Forecast System [140] and the Canadian sea ice prediction system [141] employ 3DVAR to assimilate various sea ice types for short-term sea ice forecasts. However, 3DVAR and OI have the same limitation, only considering errors in the spatial dimension, but not in the temporal dimension. That is, 3DVAR does not consider the time dependent and non-normal error in complex nonlinear dynamical models. As an extension of 3DVAR, 4DVAR can determine the modeled trajectory of sea ice state that is the best estimate of the observations and satisfies dynamical constraints of the model equations within an assimilation time window. The tangent linear and adjoint models are used to minimize the cost function within the assimilation time window. So far, little effort has been made to examine the performance of Arctic sea ice prediction through assimilating sea ice observations using 4DVAR. This is largely due to high computational cost of 4DVAR, and complication of developing and maintaining the adjoint model, which limits its application to date for complex nonlinear dynamical models.

(4) Ensemble Kalman filter (EnKF) is a flow-dependent method. It is a combination of the Kalman filter (KF) and Monte Carlo statistical method [142]. An ensemble of model state realizations is utilized to describe and propagate the estimate of model state and associated covariance matrix of the state error. The equations of the Kalman filter are given by

$$\bar{x}_a = \bar{x}_b + K\left[y_o - H\left(\bar{x}_b\right)\right],$$

$$P_a = (I - KH)P_f,$$

$$K = P_f H^T\left(HP_f H^T + R\right)^{-1}.$$

Here $\bar{x}_b$ and $\bar{x}_a$ are the ensemble mean of the model forecast and analysis, K is the Kalman gain. The matrices P_f and P_a are the ensemble-sampled model forecast and analysis covariance

matrices. The flow dependence of the EnKF arises from the fact that the ensemble of model state is propagated in time and also updated at the time when the observations are assimilated. The EnKF is relatively easy to implement because it does not need tangent linear and adjoint models to propagate error covariance. The original EnKF is a stochastic method that perturbs the observations to generate the ensemble spread in accordance with the ensemble mean error, but a number of variants of the EnKF have been developed based on either stochastic (perturbed observations) or deterministic (square root) filters. Some variants of the EnKF have been used to show their effectiveness for sea ice simulation and forecasts. Lisæter et al. [49] assimilated sea ice concentration and thickness using the original EnKF. Sea ice concentration and/or drift were assimilated in the TOPAZ4 coupled sea ice-ocean data assimilation system and the Norwegian climate prediction model using a deterministic variant of the EnKF [31,58]. A localized version of the EnKF had been used by Ref. [143] to assimilate sea ice concentration. Yang et al. [105] further assimilated both the ice concentration and thickness using the local singular evolutive Interpolated KF (LSEIKF, [144]). Chen et al. [111] used the error subspace transform ensemble KF with localization (LESTKF, [145]) to assimilate satellite-derived ice fraction and thickness. The results obtained so far showed that they have positive effects in reducing the difference between model and observations. In general, the LESTKF (ESTKF) filter is recommended if a local (global) filter is needed. The LESTKF consists of four steps: initialization, forecast, analysis, and ensemble transformation. Firstly, initial ensembles (perturbations overlaid on the mean state of model trajectories) are generated from the leading modes of the modeled sea ice state vectors, which provide an estimate of initial model states and uncertainties prior to the evolution of forecasts. Secondly, all ensembles are dynamically evolved with the model. Thirdly, the LESTKF is used to assimilate satellite sea ice parameters, considering the observational errors and background uncertainty represented by the spread of model realizations. Finally, all ensembles are transformed to new states while preserving the ensemble mean and covariance. In contrast to the original EnKF that needs observation perturbations, which can introduce sampling error that can make the analysis suboptimal, the LESTKF uses a deterministic analysis scheme.

Among the methods mentioned above, 3DVAR and variants of the EnKF are the most used methods to assimilate sea ice observations for operational sea ice forecast, and the use of EnKF has recently become more common. 3DVAR is computationally efficient, but the major disadvantage of 3DVAR is that the background error covariance is stationary in time, while large variability exists in the model forecast error. The EnKF can explicitly evolve the background error covariance through the assimilation cycle, but a major source of errors for EnKF is the sampling error due to a relatively small ensemble size, which requires to restrict the influence-distance for observations (so-called "localization") and inflation methods to avoid the underestimation of variances. To combine the complementary features of both 3DVAR and EnKF, and to address their respective issues, a hybrid ensemble and variational method, EnVAR, has been developed and is of increasing interest [146,147]. In EnVAR, the background error covariance obtained from the model ensemble is used to fully or partially replace the static background error covariance commonly used in variational methods. The Canadian regional sea ice prediction system has recently transitioned from 3DVAR to EnVAR [148] using multivariate ensemble covariance to assimilate observed sea ice fraction. While EnVAR allows to incorporate flow dependent error information into the variational data assimilation, it can also suffer from the sampling errors due to a relatively small ensemble size.

4. Discussion and summary

This paper provides a review of (1) sea ice parameters from satellite remote sensing that have been utilized and are currently under development for improved sea ice initial conditions, and (2) capabilities and limitations of different data assimilation methods that have been used to assimilate sea ice observations in dynamical models to aid in the sea ice forecast procedure.

A precondition for a meaningful assimilation of the aforementioned satellite-retrieved sea ice parameters (concentration, thickness, pond fraction, leads, and drift) into coupled predictive models is a realistic estimate of the retrieval uncertainties. For most of the observational sea ice data sets, some knowledge about their expected uncertainty exists [37,38,43,69,72,89,149]. However, most of the data sets are not distributed with uncertainty fields. Uncertainties of the satellite-retrieved sea ice parameters vary spatially and temporally. For example, uncertainties are larger in the marginal sea ice zone (low sea ice concentration, waves, flooding etc.) or under melting conditions. It is necessary to synthesize available literature and validate with airborne, buoy and mooring data to construct two or three dimensional uncertainty fields of the satellite-retrieved sea ice parameters. While these uncertainty estimates might not be correct for every single grid cell, the result still will be a vast improvement over using a single, spatially homogeneous uncertainty value for a complete data set. It is furthermore critically important that the influence of the uncertainty estimates on Arctic sea ice prediction should be examined and documented in a coordinated way, across operational and modeling centers.

The sea ice model component in most prediction systems uses categories to describe the evolution of sea ice thickness distribution within each grid cell due to both thermodynamic and dynamic processes. Each category has a value of fractional sea ice area. The total sea ice concentration of a grid cell is the sum of fractional ice areas for each category of ice. This is also true for other sea ice parameters (i.e., ice thickness, melt pond fraction). However, satellite observations only provide the aggregated value of sea ice parameters at each grid cell. Thus, a scheme is required to remap the updated aggregated sea ice parameters to ice categories after the data assimilation. Such schemes need to consider the following conservations. First, sea ice mass must be conserved when remapping the analyzed state to ice categories. This can be achieved as follows. Before assimilation, the ratios of the ice concentration (volume) in each category to the total value are stored. After assimilation, the analysis is remapped to the categories using their precalculated ratios. If the new ice thickness is larger (smaller) than the ice thickness bounds, the larger (smaller) portion is shifted to the next (previous) categories, maintaining the conservation of sea ice concentration and volume. Second, the sea ice temperature gradient in the ice layers must be maintained. This conservation is a consequence of the temperature gradient being closely related to the ice internal heat conduction, which affects the ice energy equilibrium.

Finding an appropriate method for sea ice assimilation is challenging. Unlike extensive research of data assimilation for numerical weather predictions, sea ice data assimilation is a relatively new area. Thus a rigorous intercomparison is needed to understand the performance of different assimilation methods, i.e., which method produces the most accurate analyses by effectively correcting the fast-growing errors at affordable computational cost using the same dynamical model, the same sea ice observations, the same observation error covariance matrix, and the same observation operator. Such intercomparisons can be performed using the Data Assimilation Research Testbed (DART, http://www.image.ucar.edu/DAReS/DART) and the Parallel Data Assimilation Framework (PDAF [150], http://pdaf.awi.de, a community software

providing different ensemble assimilation methods). Further, under the Joint Effort for Data assimilation Integration (JEDI) framework, a unified community data assimilation system is being developed, using a common code base. This software encompasses a variety of data assimilation methods, which would facilitate such intercomparison.

The data assimilation methods discussed above analyze variables in a Gaussian (errors are assumed to be random in nature, and follow statistically a normal distribution), which is the assumption behind the cost function. This can introduce biases for non-Gaussian variables. We know that sea ice parameters are not Gaussian distributed, i.e., the distribution of sea ice thickness features a long tail towards thicker ice in remote sensing observations [6]. In practice, the distribution of sea ice thickness is closer to a lognormal distribution, and its mean mode/median are different. Thus the distribution of sea ice parameters cannot be well represented by the Gaussian distribution. When the Gaussian-based data assimilation method is applied for non-Gaussian sea ice variables, it can make the variables unphysical, for example, introducing negative value for sea ice thickness. Fletcher and Zupanski [151,152] attempted to introduce different distributions (i.e., log-normal and mixed Gaussian-lognormal) into variational data assimilation frameworks. It is similarly necessary to consider non-Gaussian distribution of sea ice parameters in data assimilation methods, and to examine their impacts on sea ice forecast at daily to seasonal time scales.

Additionally, sea ice dynamics are highly non-linear and tightly coupled with the atmosphere and ocean. The Gaussian-based data assimilation methods have only limited abilities to handle nonlinearity in dynamical models. For this reason, there is active research in developing new filter algorithms. In particular, particle filter methods [153] are fully nonlinear, but it is still a challenge to apply them with high dimensional nonlinear models. Very recently, a few studies have demonstrated that particle filters can be applied to realistic high-dimensional models, in particular when they are applied with the method of "localization" [154,155]. While these methods should be suitable for sea ice data assimilation, none of them have yet been assessed in this context.

This review paper emphasizes the importance of assimilating satellite remote sensing of sea ice parameters into coupled predictive models to improve capability to predict Arctic sea ice. Very recently, a few studies also suggested that the incorporation of satellite-based sea surface temperature can improve hindcast of regional sea ice thickness during the melt season [156], and the assimilation of Arctic radiosonde observations can result in skillful prediction of sea ice advection driven by severe weather systems along the northern sea route [157]. Thus the assimilation of additional atmospheric and oceanic observations that strongly coupled to sea ice processes would benefit Arctic sea ice prediction [158].

Conflict of interest

The authors declare that they have no conflict of interest.

Acknowledgments

This work was supported by the National Key R&D Program of China (2018YFA0605901), the NOAA Climate Program Office (NA15OAR4310163), the National Natural Science Foundation of China (41676185), and the Key Research Program of Frontier Sciences of Chinese Academy of Sciences (QYZDY-SSW-DQC021).

Appendix A. Supplementary data

Supplementary data to this article can be found online at https://doi.org/10.1016/j.scib.2018.11.018.

References

[1] Polyak L, Alley R, Andrews J, et al. History of sea ice in the Arctic. Quat Sci Rev 2010;29:1757–78.
[2] Meier W, Stroeve J, Barrett A, et al. A simple approach to providing a more consistent Arctic sea ice extent time series from the 1950s to present. Cryosphere 2012;6:1359–68.
[3] Cavalieri D, Parkinson C. Arctic sea ice variability and trends, 1979–2010. Cryosphere 2012;6:881–9.
[4] Stroeve J, Kattsov V, Barrett A, et al. Trends in Arctic sea ice extent from CMIP5, CMIP3 and observations. Geophys Res Lett 2012;39:L16502.
[5] Kwok R, Rothrock D. Decline in Arctic sea ice thickness from submarine and ICESat records 1958–2008. Geophys Res Lett 2009;36:L15501.
[6] Kwok R, Cunningham G. Variability of Arctic sea ice thickness and volume from CryoSat-2. Phil Trans R Soc Ser A Math Phys Eng Sci 2015;373:2045.
[7] Maslanik J, Stroeve J, Fowler C, et al. Distribution and trends in Arctic sea ice age through spring 2011. Geophys Res Lett 2011;38:L13502.
[8] Comiso J. Large decadal decline of the Arctic multiyear ice cover. J Clim 2012;25:1176–93.
[9] Rampal P, Weiss J, Marsan D. Positive trend in the mean speed and deformation rate of Arctic sea ice 1979–2007. J Geophys Res 2009;114:C05013.
[10] Spreen G, Kwok R, Menemenlis D. Trends in Arctic sea ice drift and role of wind forcing: 1992–2009. Geophys Res Lett 2011;38:L19501.
[11] Kwok R, Spreen G, Pang S. Arctic sea ice circulation and drift speed: decadal trends and ocean currents. J Geophys Res 2013;118:2408–25.
[12] Smith L, Stephenson S. New Trans-Arctic shipping routes navigable by midcentury. Proc Natl Acad Sci USA 2013;110:E1191–5.
[13] World Weather Research Programme (WWRP)/Polar Prediction Project (PPP) implementation plan; 2014 https://www.polarprediction.net/fileadmin/user_upload/www.polarprediction.net/Home/Documents/WWRP-PPP_IP_Final_12Jan2013_v1_2.pdf.
[14] Melia N, Haines K, Hawkins E. Sea ice decline and 21st century trans-Arctic shipping routes. Geophys Res Lett 2016;43:9720–8.
[15] Newton R, Pfirman S, Schlosser P, et al. White Arctic vs. Blue Arctic: a case study of diverging stakeholder responses to environmental change. Earth Future 2016;4:396–405.
[16] Stroeve J, Hamilton L, Bitz C, et al. Predicting September sea ice: ensemble skill of the SEARCH Sea Ice Outlook 2008–2013. Geophys Res Lett 2014;41:2411–8.
[17] Ono J, Inoue J, Yamazaki A, et al. The impact of radiosonde data on forecasting sea-ice distribution along the Northern Sea Route during an extremely developed cyclone. J Adv Model Earth Syst 2016;8:292–303.
[18] Liu J, Curry J, Wang H, et al. Impact of declining Arctic sea ice on winter snowfall. Proc Natl Acad Sci USA 2012;109:4074–9.
[19] Francis J, Vavrus S. Evidence linking Arctic amplification to extreme weather in mid-latitudes. Geophys Res Lett 2012;39:L06801.
[20] Mori M, Watanabe M, Shiogama H, et al. Robust Arctic sea-ice influence on the frequent Eurasian cold winters in past decades. Nat Geosci 2014;7:869–73.
[21] Cohen J, Screen J, Furtado J, et al. Recent Arctic amplification and extreme mid-latitude weather. Nat Geosci 2014;7:627–37.
[22] National Research Council. Linkages between Arctic warming and mid-latitude weather patterns: summary of a workshop. Washington DC: The National Academies Press; 2014.
[23] Overland J. Is the melting Arctic changing midlatitude weather? Phys Today 2016;69:38.
[24] Overland J, Wang M. When will the summer Arctic be nearly sea ice free? Geophys Res Lett 2013;40:2097–101.
[25] Liu J, Song M, Horton R, et al. Reducing spread in climate model projections of a September ice-free Arctic. Proc Natl Acad Sci USA 2013;110:12571–6.
[26] Notz D, Stroeve J. Observed Arctic sea-ice loss directly follows anthropogenic CO_2 emission. Science 2016;354:747–50.
[27] Yang S, Dong W, Feng J, et al. Global warming projections using the human-earth system model BNUHESM1.0. Sci Bull 2016;61:1833–8.
[28] Zhang J, Steele M, Lindsay A, et al. Ensemble one-year predictions of arctic sea ice for the spring and summer of 2008. Geophys Res Lett 2008;35:L08502.
[29] Hebert D, Allard R, Metzger E, et al. Short-term sea ice forecasting: an assessment of ice concentration and ice drift forecasts using the US Navy's Arctic Cap Nowcast/Forecast System. J Geophys Res 2015;120:8327–45.
[30] Buehner M, Caya A, Pogson L, et al. A new environment Canada regional ice analysis system. Atmos Ocean 2013;51:18–34.
[31] Sakov P, Counillon F, Bertino L, et al. TOPAZ4: an ocean-sea ice data assimilation system for the North Atlantic and Arctic. Ocean Sci 2012;8:633–56.
[32] Saha S, Moorthi S, Wu X, et al. The NCEP climate forecast system version 2. J Clim 2014;27:2185–208.
[33] Rienecker M, Suarez M, Todling R, et al. In: The GEOS-5 data assimilation system - documentation of versions 5.0.1, 5.1.0, and 5.2.0. Technical report series on global modeling and data assimilation. p. 27.
[34] MacLachlan C, Arribas A, Peterson K, et al. Description of GloSea5: the Met Office high resolution seasonal forecast system. Quart J Roy Meteorol Soc 2015;141:1072–84.
[35] Guemas V, Blanchard-Wrigglesworth E, Chevallier M, et al. A review on Arctic sea ice predictability and prediction on seasonal to decadal time-scales. Quart J Roy Meteorol Soc 2014;142:546–61.

[36] Jung T, Gordon N, Bauer P, et al. Advancing polar prediction capabilities on daily to seasonal time scales. Bull Am Meteorol Soc 2016;97:1631–47.
[37] Ivanova N, Johannessen O, Pedersen L, et al. Retrieval of Arctic sea ice parameters by satellite passive microwave sensors: a comparison of eleven sea ice concentration algorithms. IEEE Trans Geosci Remote Sens 2014;52:7233–46.
[38] Ivanova N, Pedersen L, Tonboe T, et al. Inter-comparison and evaluation of sea ice algorithms: towards further identification of challenges and optimal approach using passive microwave observations. Cryosphere 2015;9:1797–817.
[39] Swift C, Fedor L, Ramseier R. An algorithm to measure sea ice concentration with microwave radiometers. J Geophys Res 1985;90:1087–99.
[40] Maslanik J, Stroeve J. Near-real-time DMSP SSMIS daily polar gridded sea ice concentrations, version. 1 National Snow and Ice Data Center; 1999. updated daily.
[41] Meier W, Peng G, Scott D, et al. Verification of a new NOAA/NSIDC passive microwave sea-ice concentration climate record. Polar Res 2014;33:21004.
[42] Meier W, Fetterer F, Windnagel A. Near-real-time NOAA/NSIDC climate data record of passive microwave sea ice concentration, version 1, 2017.
[43] Spreen G, Kaleschke L, Heygster G. Sea ice remote sensing using AMSR-E 89 GHz channels. J Geophys Res 2008;113:C02S03.
[44] Tonboe R, Lavelle J, Pfeiffer R, et al. Product user manual for OSI SAF global sea ice concentration. Copenhagen: Danish Meteorological Institutes; 2016.
[45] Thomas D, Rothrock D. Blending sequential scanning multichannel microwave radiometer and buoy data into a sea ice model. J Geophys Res 1989;94:10907–20.
[46] Thomas D, Rothrock D. The Arctic Ocean ice balance: a Kalman smoother estimate. J Geophys Res 1993;98:10053–67.
[47] Thomas D, Martin S, Rothrock D, et al. Assimilating satellite concentration data into an Arctic sea ice mass balance model, 1979–1985. J Geophys Res 1996;101:20849–68.
[48] Duliere V, Fichefet T. On the assimilation of ice velocity and concentration data into large-scale sea ice models. Ocean Sci 2007;3:321–35.
[49] Lisæter K, Rosanova J, Evensen G. Assimilation of ice concentration in a coupled ice-ocean model, using the Ensemble Kalman filter. Ocean Dyn 2003;53:368–88.
[50] Van Woert M, Zou C, Meier W, et al. Forecast verification of the polar ice prediction system (PIPS) sea ice concentration fields. J Atmos Oceanic Technol 2004;21:944–57.
[51] Lindsay R, Zhang J. Assimilation of ice concentration in an ice-ocean model. J Atmos Oceanic Technol 2006;23:742–9.
[52] Stark J, Ridley J, Martin M, et al. Sea ice concentration and motion assimilation in a sea ice-ocean model. J. Geophys Res 2008;113:C05S91.
[53] Wang K, Debernard J, Sperrevik A, et al. A combined optimal interpolation and nudging scheme to assimilate OSISAF sea ice concentration in ROMS. Ann Glaciol 2013;54:8–12.
[54] Yang Q, Losa N, Losch M, et al. Assimilating summer sea ice concentration into a coupled ice-ocean model using a localized SEIK filter. Ann Glaciol 2015;56:38–44.
[55] Toyoda T, Fujii Y, Yasuda T, et al. Data assimilation of sea ice concentration into a global ocean-sea ice model with corrections for atmospheric forcing and ocean temperature fields. J Oceanogr 2016;72:235–62.
[56] Wang W, Chen M, Kumar A. Seasonal prediction of arctic sea ice extent from a coupled dynamical forecast system. Mon Weather Rev 2013;141:1375–94.
[57] Tietsche S, Notz D, Jungclaus J, et al. Assimilation of sea-ice concentration in a global climate model – physical and statistical aspects. Ocean Sci 2013;9:19–36.
[58] Kimmritz M, Counillon F, Bitz C, et al. Optimising assimilation of sea ice concentration in an Earth system model with a multicategory sea ice model. Tellus A Dyn Meteorol Oceanogr 2018;70:1435945.
[59] Bunzel F, Notz D, Baehr J, et al. Seasonal climate forecasts significantly affected by observational uncertainty of Arctic sea ice concentration. Geophys Res Lett 2016;43:852–9.
[60] Tonboe R, Nielsen E OSI-409. In: Global sea ice concentration reprocessing validation report. Eumetsat Osi Saf Prod Rep 2010;18. p. 18.
[61] Yang Q, Losch M, Losa S, et al. Brief communication: the challenge and benefit of using sea ice concentration satellite data products with uncertainty estimates in summer sea ice data assimilation. Cryosphere 2016;10:761–74.
[62] Lavergne T, Sørensen A, Kern S, et al. Version 2 of the EUMETSAT OSI SAF and ESA CCI sea ice concentration climate data records. Cryosphere Discuss 2018. https://doi.org/10.5194/tc-2018-127.
[63] Olason E, Notz D. Drivers of variability in Arctic sea-ice drift speed. J Geophys Res 2014;119:5755–75.
[64] Kwok R. Summer sea ice motion from the 18 GHz channel of AMSR-E and the exchange of sea ice between the Pacific and Atlantic sectors. Geophys Res Lett 2008;35:L03504.
[65] Girard-Ardhuin F, Ezraty R. Enhanced Arctic sea ice drift estimation merging radiometer and scatterometer data. IEEE Trans Geosci Remote Sens 2012;50:2639–48.
[66] Fowler C, Emery W, Tschudi M. Polar Pathfinder daily 25 km EASE-Grid sea ice motion vectors, version 2. NSIDC; 2013.
[67] Kwok R, Cunningham G. Seasonal ice area and volume production of the Arctic Ocean: November 1996 through April 1997. J Geophys Res 2002;107:8038.
[68] Korosov A, Rampal P. A combination of feature tracking and pattern matching with optimal parameterization for sea ice drift retrieval from SAR Data. Remote Sens 2017;9:258.
[69] Sumata H, Lavergne T, Girard-Ardhuin F, et al. An intercomparison of arctic ice drift products to deduce uncertainty estimates. J Geophys Res 2014;119:4887–921.
[70] Lavergne T, Eastwood S, Teffah Z. Sea ice motion from low-resolution satellite sensors: an alternative method and its validation in the Arctic. J Geophys Res 2010;115:C10032.
[71] Girard-Ardhuin F, Ezraty R, Croizé-Fillon D, et al. Sea ice drift in the Central Arctic combing Quikscat and Ssmi/I sea ice Drift Data–User'S Manual Version 3.0. Brest, France: IFREMER; 2008.
[72] Sumata H, Gerdes R, Kauker F, et al. Empirical error functions for monthly mean Arctic sea-ice drift. J Geophys Res 2015;120:7450–75.
[73] Meier W, Maslanik J, Fowler C. Error analysis and assimilation of remotely sensed ice motion within an Arctic sea ice model. J Geophys Res 2000;105:3339–56.
[74] Meier W, Maslanik J. Improved sea ice parcel trajectories in the Arctic via data assimilation. Mar Pollut Bull 2001;42:505–11.
[75] Meier W, Maslanik J. Effect of environmental conditions on observed, modeled, and assimilated sea ice motion errors. J Geophys Res 2003;108:1–11.
[76] Arbetter T, Lynch A, Maslanik J, et al. Effects of data assimilation of ice motion in a basin-scale sea ice model, in ice in the environment. In: Squire V, Langhore P, editors. Proceedings of the 16th IAHR international symposium on ice. p. 186–93.
[77] Dai M, Arbetter T, Meier W. Data assimilation of sea ice motion vectors: sensitivity to the parameterization of sea ice strength. Ann Glaciol 2006;44:357–60.
[78] Rollenhagen K, Timmermann R, Janjic T, et al. Assimilation of sea ice motion in a finite-element sea ice model. J Geophys Res 2009;114:C05007.
[79] Zhang J, Thomas D, Rothrock D, et al. Assimilation of ice motion observations and comparisons with submarine ice thickness data. J Geophys Res 2003;108:3170.
[80] Spreen G, Kwok R, Menemenlis D, et al. Sea-ice deformation in a coupled ocean-sea-ice model and in satellite remote sensing data. Cryosphere 2017;11:1553–73.
[81] Rampal P, Bouillon S, Olason E, et al. neXtSIM: a new Lagrangian sea ice model. Cryosphere 2016;10:1055–73.
[82] Yang CY, Liu J, Hu Y, et al. Assessment of Arctic and Antarctic sea ice predictability in CMIP5 Decadal Hindcasts. Cryosphere 2016;10:2429–52.
[83] Nakanowatari T, Inoue J, Sato K, et al. Medium-range predictability of early summer sea ice thickness distribution in the East Siberian Sea based on the TOPAZ4 ice-ocean data assimilation system. Cryosphere 2018;12:2005–20.
[84] Blanchard-Wrigglesworth E, Armour K, Bitz C, et al. Persistence and inherent predictability of Arctic sea ice in a GCM ensemble and observations. J Clim 2011;24:231–50.
[85] Chevallier M, Salas-Melia D. The role of sea ice thickness distribution in the Arctic sea ice potential predictability: a diagnostic approach with a coupled GCM. J Clim 2012;25:3025–37.
[86] Day J, Hawkins E, Tietsche S. Will Arctic sea ice thickness initialization improve seasonal forecast skill? Geophys Res Lett 2014;41:7566–75.
[87] Kwok R. Satellite remote sensing of sea ice thickness and kinematics: a review. J Glaciol 2010;56:1129–40.
[88] Laxon S, Giles K, Ridout A, et al. CryoSat-2 estimates of Arctic sea ice thickness and volume. Geophys Res Lett 2013;40:732–7.
[89] Ricker R, Hendricks S, Helm V, et al. Sensitivity of CryoSat-2 Arctic sea-ice freeboard and thickness on radar-waveform interpretation. Cryosphere 2014;8:1607–22.
[90] Armitage T, Ridout A. Arctic sea ice freeboard from AltiKa and comparison with CryoSat-2 and Operation IceBridge. Geophys Res Lett 2015;42:6724–31.
[91] Maaß N, Kaleschke L, Tian-Kunze X, et al. Snow thickness retrieval over thick Arctic sea ice using SMOS satellite data. Cryosphere 2013;7:1971–89.
[92] Sato K, Inoue J. Comparison of Arctic sea ice thickness and snow depth estimates from CFSR with *in situ* observations. Clim Dyn 2018;50:289–301.
[93] Kaleschke L, Tian-Kunze X, Maaß N, et al. Sea ice thickness retrieval from SMOS brightness temperatures during the Arctic freeze-up period. Geophys Res Lett 2012;39:L05501.
[94] Tian-Kunze X, Kaleschke L, Maaß N, et al. SMOS-derived thin sea ice thickness: algorithm baseline, product specifications and initial verification. Cryosphere 2014;8:997–1018.
[95] Huntemann M, Heygster G, Kaleschke L, et al. Empirical sea ice thickness retrieval during the freeze-up period from SMOS high incident angle observations. Cryosphere 2014;8:439–51.
[96] Patilea C, Heygster G, Huntemann M, et al. Combined SMAP/SMOS thin sea ice thickness retrieval. Cryosphere 2017. https://doi.org/10.5194/tc-2017-168.
[97] Schmitt A, Kaleschke L. A consistent combination of brightness temperatures from SMOS and SMAP over polar oceans for sea ice applications. Remote Sens 2018;10:553.
[98] Ricker R, Hendricks S, Kaleschke L, et al. A weekly Arctic sea-ice thickness data record from merged CryoSat-2 and SMOS satellite data. Cryosphere 2017;11:1607–23.
[99] Kurtz N, Galin N, Studinger M. An improved CryoSat-2 sea ice freeboard retrieval algorithm through the use of waveform fitting. Cryosphere 2014;8:1217–37.

[100] Kurtz N, Harbeck J. CryoSat-2 Level-4 sea ice elevation, freeboard, and thickness, version 1. National Snow and Ice Data Center; 2017.
[101] Grosfeld K, Treffeisen R, Asseng J, et al. Online sea-ice knowledge and data platform <www.meereisportal.de>. Polarforschung 2016;85:143–55.
[102] Tian-Kunze X, Kaleschke L, Maass NSMOS. Daily sea ice thickness version 3, ICDC, icdc.cen.uni-hamburg.de. Germany: University of Hamburg; 2016.
[103] Lisæter K, Evensen G, Laxon S. Assimilating synthetic CryoSat sea ice thickness in a coupled ice-ocean model. J Geophys Res 2007;112:C07023.
[104] Lindsay R, Haas C, Hendricks S, et al. Seasonal forecasts of Arctic sea ice initialized with observations of ice thickness. Geophys Res Lett 2012;39:L21502.
[105] Yang Q, Losa S, Losch M, et al. Assimilating SMOS sea ice thickness into a coupled ice-ocean model using a local SEIK filter. J Geophys Res 2014;119:6680–92.
[106] Yang Q, Losch M, Loza S, et al. Taking into account atmospheric uncertainty improves sequential assimilation of SMOS sea ice thickness data in an ice-ocean model. J Atmos Oceanic Technol 2016;33:397–407.
[107] Xie J, Counillon F, Bertino L, et al. Benefits of assimilating 5 thin sea ice thickness from SMOS into the TOPAZ system. Cryosphere 2016;10:2745–61.
[108] Mu L, Yang Q, Losch M, et al. Improving sea ice thickness estimates by assimilating CryoSat-2 and SMOS sea ice thickness data simultaneously. Quart J Roy Meteorol Soc 2018;144:529–38.
[109] Allard R, Farrell S, Hebert D, et al. Utilizing CryoSat-2 sea ice thickness to initialize a coupled ice-ocean modeling system. Adv Space Res 2018;62:1265–80.
[110] Collow T, Wang W, Kumar A, et al. Improving Arctic sea ice prediction using PIOMAS initial sea ice thickness in a coupled ocean-atmosphere model. J Clim 2015;143:4618–30.
[111] Chen Z, Liu J, Song M, et al. Impacts of assimilating satellite sea ice concentration and thickness on Arctic sea ice prediction in the NCEP climate forecast system. J Clim 2017;30:8429–46.
[112] Zhang J, Rothrock D. Modeling global sea ice with a thickness and enthalpy distribution model in generalized curvilinear coordinates. Mon Weather Rev 2003;131:845–61.
[113] Xie J, Counillon F, Bertino L. Impact of assimilating a merged sea ice thickness from CryoSat-2 and SMOS in the Arctic reanalysis. Cryosphere Discuss 2018. https://doi.org/10.5194/tc-2018-101.
[114] Mu L, Losch M, Yang Q, et al. Arctic-wide sea-ice thickness estimates from combining satellite remote sensing data and a dynamic ice-ocean model with data assimilation during the CryoSat-2. J Geophys Res 2018. https://doi.org/10.1029/2018JC014316.
[115] Polashenski C, Perovich D, Courville Z. The mechanisms of sea ice melt pond formation and evolution. J Geophys Res 2012;117:C01001.
[116] Hunke E, Hebert D, Lecomte O. Level-ice melt ponds in the Los Alamos sea ice model, CICE. Ocean Model 2013;71:26–42.
[117] Curry J, Schramm J, Ebert E. On the sea ice albedo climate feedback mechanism. J Clim 1995;8:240–7.
[118] Perovich D, Grenfell T, Light B, et al. Trans-polar observations of the morphological properties of Arctic sea ice. J Geophys Res 2009;114:C00A04.
[119] Dou T, Xiao C, Du Z, et al. Sources, evolution and impacts of EC and OC in snow on sea ice: a measurement study in Barrow, Alaska. Sci Bull 2017;62:1547–54.
[120] Nicolaus M, Katlein C, Maslanik J, et al. Changes in Arctic sea ice result in increasing light transmittance and absorption. Geophys Res Lett 2012;39:L24501.
[121] Nicolaus M, Katlein C. Mapping radiation transfer through sea ice using a remotely operated vehicle (ROV). Cryosphere 2013;7:763–77.
[122] Inoue J, Kikuchi T, Perovich D. Effect of heat transmission through melt ponds and ice on melting during summer in the Arctic Ocean. J Geophys Res 2008;113:C05020.
[123] Schroder D, Feltham D, Flocco D, et al. September Arctic sea-ice minimum predicted by spring melt-pond fraction. Nat Clim Change 2014;4:353–7.
[124] Liu J, Song M, Horton R, et al. Revisiting the potential of melt pond fraction as a predictor for the seasonal Arctic sea ice minimum. Environ Res Lett 2015;10:054017.
[125] Rösel A, Kaleschke L, Birnbaum G. Melt ponds on Arctic sea ice determined from MODIS satellite data using an artificial neural network. Cryosphere 2012;6:31–46.
[126] Zege E, Malinka A, Katsev I, et al. Algorithm to retrieve the melt pond fraction and the spectral albedo of Arctic summer ice from satellite optical data. Remote Sens Environ 2015;163:153–64.
[127] Istomina L, Heygster G, Huntemann M, et al. Melt pond fraction and spectral sea ice albedo retrieval from MERIS data – Part 1: validation against *in situ*, aerial, and ship cruise data. Cryosphere 2015;9:1551–66.
[128] Malinka A, Zege E, Istomina L, et al. Reflective properties of melt ponds on sea ice. Cryosphere 2018;12:1921–37.
[129] Andreas E, Paulson C, William R, et al. The turbulent heat flux from Arctic leads. Bound Lay Meteorol 1979;17:57–91.
[130] Andreas E, Cash B. Convective heat transfer over wintertime leads and polynyas. J Geophys Res 1999;104:25721–34.
[131] Marcq S, Weiss J. Influence of sea ice lead-width distribution on turbulent heat transfer between the ocean and the atmosphere. Cryosphere 2012;6:143–56.
[132] Ledley T. A coupled energy balance climate-sea ice model: impact of sea ice and leads on climate. J Geophys Res 1988;93:15919–32.
[133] Zhang Y, Cheng X, Liu J, et al. The potential of sea ice leads as a predictor for seasonal Arctic sea ice extent prediction. Cryosphere 2018. https://doi.org/10.5194/tc-2018-108.
[134] Röhrs J, Kaleschke L. An algorithm to detect sea ice leads by using AMSR-E passive microwave imagery. Cryosphere 2012;6:343–52.
[135] Willmes S, Heinemann G. Pan-Arctic lead detection from MODIS thermal infrared imagery. Ann Glaciol 2015;56:29–37.
[136] Willmes S, Heinemann G. Sea-ice wintertime lead frequencies and regional characteristics in the Arctic, 2003–2015. Remote Sens 2016;8:4.
[137] Blockley E, Peterson K. Improving met office seasonal forecasts of Arctic sea ice using assimilation of CryoSat-2 thickness. Cryosphere Discuss 2018;12:3419–38.
[138] Derber J, Rosati A. A global oceanic data assimilation system. J Phys Oceanogr 1989;19:1333–47.
[139] Caya A, Buehner M, Carrieres T. Analysis and forecasting of sea ice conditions in three dimensional variational data assimilation and a coupled ice-ocean model. J Atmos Oceanic Technol 2010;27:353–69.
[140] Hebert D, Allard R, Metzger E, et al. Short-term sea ice forecasting: an assessment of ice concentration and ice drift forecasts using the U.S. Navy's Arctic Cap Nowcast/ForecastSystem. J Geophys Res 2015;120:8327–45.
[141] Lemieux J, Beaudoin C, Dupont F, et al. The regional ice prediction system (RIPS): verification of forecast sea ice concentration. Quart J Roy Meteorol Soc 2016;142:632–43.
[142] Evensen G. Sequential data assimilation with a nonlinear quasi-geostrophic model using Monte Carlo methods to forecast error statistics. J Geophys Res 1994;99:10143–62.
[143] Massonnet F, Fichefetc T, Goosse H. Prospects for improved seasonal Arctic sea ice predictions from multivariate data assimilation. Ocean Model 2015;88:16–25.
[144] Nerger L, Danilov S, Hiller W, et al. Using sea-level data to constrain a finite-element primitive-equation ocean model with a local SEIK filter. Ocean Dyn 2006;56:634–49.
[145] Nerger L, Janjić T, Schröter J, et al. A unification of ensemble square root Kalman filters. Mon Weather Rev 2012;140:2335–45.
[146] Desroziers G, Camino J, Berre L. 4DenVar: link with 4D state formulation of variational assimilation and different possible implementations. Quart J Roy Meteorol Soc 2014;14:2097–110.
[147] Lorenc A, Bowler N, Clayton A, et al. Comparison of hybrid-4denvar and hybrid-4dvar data assimilation methods for global NWP. Mon Weather Rev 2015;143:212–29.
[148] Shlyaeva A, Buehner M, Caya A, et al. Towards ensemble data assimilation for the environment Canada Regional Ice Prediction System. Quart J Roy Meteorol Soc 2016;142:1090–9.
[149] Kern S, Spreen G. Uncertainties in Antarctic Sea-Ice thickness retrieval from ICESat. Ann Glaciol 2015;56:107–19.
[150] Nerger L, Hiller W. Software for ensemble-based data assimilation systems-implementation strategies and scalability. Comp Geosci 2013;55:110–8.
[151] Fletcher S, Zupanski M. A data assimilation method for lognormally distributed observational errors. Quart J Roy Meteorol Soc 2006;132:2505–19.
[152] Fletcher S, Zupanski M. Implications and impacts of transforming lognormal variables into normal variables in VAR. Meteor Z 2007;16:755–65.
[153] Van Leeuwen P. Particle filtering in geophysical systems. Mon Weather Rev 2009;137:4089–114.
[154] Tödter J, Kirchgessner P, Nerger L, et al. Assessment of a nonlinear ensemble transform filter for high-dimensional data assimilation. Mon Weather Rev 2016;144:409–27.
[155] Poterjoy J, Anderson J. Efficient assimilation of simulated observations in a high-dimensional geophysical system using a localized particle filter. Mon Weather Rev 2016;144:2007–20.
[156] Zheng F, Zhu J. Coupled assimilation for an intermediated coupled ENSO prediction model. Ocean Dyn 2010;60:1061–73.
[157] Liang X, Yang Q, Nerger L, et al. Assimilating Copernicus SST data into a pan-Arctic ice-ocean coupled model with a local SEIK filter. J Atmos Oceanic Technol 2017;34:1985–99.
[158] Inoue J, Yamazaki A, Ono J, et al. Additional Arctic observations improve weather and sea-ice forecasts for the Northern Sea Route. Sci Rep 2015;5:16868.

Jiping Liu is a professor of Department of Atmospheric and Environmental Sciences, University at Albany, State University of New York. His research focuses on polar climate variability and change, in particular sea ice variability, modeling, and prediction, Arctic change and mid-latitude weather and climate, and remote sensing in sea ice and ocean.